Detecting Signals With Direct Fast Fourier Transform for Microarray Data Collection

Ru Chen, Chenggang Zhu, Bilin Ge, Xiangdong Zhu, Yung-Shin Sun, Lan Mi, Jiong Ma, Xu Wang, and Yiyan Fei

***Abstract*— Small signals are routinely detected at a frequency away from the 1/f noise. Typically, the signal source is modulated at a suitable frequency, and the harmonics of the modulation frequency in the signal are analyzed with phase sensitive detectors such as Lock-in amplifiers. Yet, the high cost and poor portability of stand-alone Lock-in amplifiers are obstacles to making such an approach of harmonic detection into a widely usable instrumentation. In this letter, we show that for many applications where signals are not too small (e.g., more than tens of micro-volts) the direct fast Fourier transform using a commercially available, general-purpose data acquisition board serves as a cost-effective alternative to Lock-in amplifiers without sacrificing the signal-to-noise ratio.**

***Index Terms*— Fast Fourier transform, lock-in amplifier, microarray detection, optical biosensor.**

I. Introduction

AT FRONTIERS of physical measurements, more often than not one encounters challenges of detecting many small signals in the range of nV to μV simultaneously. To avoid the 1/f noise that plagues measurements at low frequency, one routinely finds ways to modulate the signal source at a desirable frequency and detects the resulting signal that now varies with time periodically. In these cases, phase-sensitive detectors such as Lock-in amplifiers are used to obtain various harmonics of the modulation frequency in the signal. A Lock-in amplifier is effectively a Fourier analyzer that yields information on one harmonic at a time. The advantages of Lock-in amplifier are its capabilities 1) to detect a small periodic signal on top of a large DC background; 2) to amplify signals as small as nV to the range of V with low noise amplifiers before Fourier analysis; 3) to yield the phase as well as the amplitude of a harmonic component; 4) to offer the convenience of a stand-alone, user-friendly instrument. The disadvantages of Lock-in amplifiers are also obvious: i) each unit only measures one harmonic in the signal at a time and if multiple harmonics are simultaneously needed, as many Lock-in amplifiers are required; ii) they are bulky and expensive apparatus that are neither economical nor convenient to serve as integral parts of a widely usable instrumentation. Kapitulnik and coworkers developed a Sagnac interferometry in which two counter propagating beams are modulated with an electro-optic phase modulator at a high frequency but at a delayed time [1]. The suitable interference of the two beams is detected with a photo-receiver and the output of the receiver is analyzed with a pair of Lock-in amplifiers to extract magnitudes of the first and the second harmonics in modulation frequency. The ratio of the two harmonics yields the time-reversal symmetry breaking effect along the optical path while removing effects of the intensity drift and the throughput of the beams. Similarly Zhu and coworkers developed a special form of ellipsometry that measures the oblique-incidence reflectivity difference (OI-RD) arising from an ultrathin film on a solid substrate [2]. Essential parts of an OI-RD system include a laser and a photo-elastic modulator (PEM). PEM alters the polarization state of the laser beam at a frequency (f_{PEM} = 50 kHz). After the beam is reflected from a thin-film-covered substrate surface, the light beam is detected with a photo-receiver. The output of the receiver is typically analyzed with two Lock-in amplifiers which measure respectively the first and the second harmonics of the modulation frequency in the photocurrent. Again the ratio of the first harmonic amplitude to the second harmonic amplitude yields the OI-RD signal [2], a step that removes effects of the beam intensity drift and the throughput of the optical system [2]–[8]. However, much broader application of OI-RD including the development of a commercially viable instrumentation is hindered by the practical limitation associated with the use of bulky and expensive Lock-in amplifiers [9], [10]. Interestingly signals in most OI-RD measurements are tens of μV to mV instead of a few μV or lower, the wide range of gain offered by a Lock-in amplifier is not really needed. The phase information available from a standard Lock-in amplifier is not needed either. Furthermore, noises in OI-RD measurements are usually dominated by the temporal variation of the birefringence in the optical system. As a result, it is sensible to explore the option of harmonic measurement using discrete Fourier transform (DFT) [11]. The main advantage of such an alternative is that one can measure magnitudes of multiple harmonics without the bulky costly Lock-in amplifiers.

Manuscript received August 29, 2017; revised October 18, 2017; accepted October 29, 2017. Date of publication November 8, 2017; date of current version November 17, 2017. This work was supported in part by the National Natural Science Foundation of China under Grant 61505032, Grant 11574056, Grant 61575046, and Grant 31500599, in part by the Open Foundation of the State Key Laboratory of Modern Optical Instrumentation, in part by Qing Lan Project under Grant BT2015-10, and in part by the Scientific Research Foundation of WXIT under Grant 3115006931. *(Corresponding authors: Yiyan Fei; Xu Wang.)*

R. Chen, C. Zhu, B. Ge, L. Mi, J. Ma, and Y. Fei are with the Key Laboratory of Micro and Nano Photonic Structures (Ministry of Education), Shanghai Engineering Research Center of Ultra-Precision Optical Manufacturing, Green Photoelectron Platform, Department of Optical Science and Engineering, Fudan University, Shanghai 200433, China (e-mail: fyy@fudan.edu.cn).

X. Zhu is with the Department of Physics, University of California at Davis, Davis, CA 95616 USA.

Y.-S. Sun is with the Department of Physics, Fu Jen Catholic University, New Taipei City 24205, Taiwan.

X. Wang is with the Department of Fundamental Courses, Wuxi Institute of Technology, Wuxi 214121, China (e-mail: wangxu@wxit.edu.cn).

Digital Object Identifier 10.1109/LPT.2017.2771344

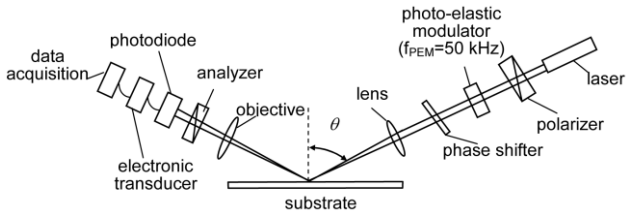

Fig. 1. Schematic diagram of an oblique-incidence reflectivity difference (OI-RD) system for thin film characterization.

In this work, we compare measurements of an OI-RD signal in mV range using both the conventional Lock-in amplifier method and the direct Fast Fourier transform (FFT). The results demonstrate that a direct FFT-based method for measuring harmonics of small periodic signal is indeed a viable alternative to the Lock-in amplifier based approach. In particular, we show that the direct FFT approach yields amplitudes of harmonics with comparable signal-to-noise ratio as achieved with stand-alone Lock-in amplifiers over the same acquisition time.

II. Principles and Experimental Setup

A. Small Oscillatory Signals Produced in an OI-RD Detection System

Fig. 1 shows the schematic of an oblique-incidence reflectivity (OI-RD) detection system. With the polarization state of an incident laser beam modulated by a photoelastic modulator (PEM) at the frequency f_{PEM}, the light beam intensity at the photo-receiver consists of harmonics of the modulation frequency [2] as follows,

$$\begin{aligned} I(t) = I_{dc} &+ I_1 \cos(2\pi f_{PEM} t + \varphi_1) \\ &+ I_2 \cos(2\pi \cdot 2 f_{PEM} t + \varphi_2) + \text{higher harmonics} \end{aligned} \quad (1)$$

φ_1 and φ_2 are phases for the harmonic components. I_1 and I_2 are amplitudes of the first and second harmonic components, respectively. They are functions of the physical property of a thin layer on the solid substrate as [2]

$$I_1 = -I_0 \eta_1 J_1(\varphi_A) |r_p| |r_s| \sin(\delta - \delta_0) \quad (2)$$

$$I_2 = I_0 \eta_2 J_2(\varphi_A) |r_p| |r_s| \cos(\delta - \delta_0) \quad (3)$$

$$\begin{aligned} \Delta\delta = \delta - \delta_0 &= \left| \frac{I_1 J_2(\varphi_A) \eta_2}{I_2 J_1(\varphi_A) \eta_1} \right| \\ &\cong \frac{-4\pi \sqrt{\varepsilon_s} \cos\theta}{(\varepsilon_0 - \varepsilon_s)\left(\cot^2\theta - \varepsilon_s/\varepsilon_0\right)} \frac{(\varepsilon_d - \varepsilon_o)(\varepsilon_d - \varepsilon_s)}{\varepsilon_d} \frac{d}{\lambda} \end{aligned} \quad (4)$$

I_0 is the initial intensity of the incident beam. η_1 and η_2 are amplification factors at the two harmonics. $J_1(\varphi_A)$ and $J_2(\varphi_A)$ are Bessel functions of the first kind. φ_A is the amplitude of the modulation in the PEM. $\varepsilon_s, \varepsilon_0$, and ε_d are optical dielectric constants of the ambient, the solid substrate, and the ultrathin film, respectively. θ is the incident angle. $|r_p|$ and $|r_s|$ are reflectivities for p- and s-polarized components of the light beam off the solid substrate when it is covered with an ultrathin film. δ_0 and δ are the phase difference between the p- and s-polarization from the bare substrate and substrate bearing samples, respectively. In OI-RD, one measures the molecular thickness d through the detection of $\Delta\delta$.

When the OI-RD signal is analyzed with a pair of Lock-in amplifiers, the equivalent noise bandwidth (ENBW) $\Delta f_{Lock\text{-}in}$ is determined by the slope of the low pass filter and the time constant T. The wait time for the signal to reach the 99% of its final value serves as the effective sampling time τ_{wait}. It is given by $\tau_{wait} \approx 1/\Delta f_{Lock\text{-}in}$ in practice. For example, with a low pass filter having a slope of 24 dB/oct and a time constant $T = 100\ \mu s$, $\Delta f_{Lock\text{-}in} = 5/(64T)$ and $\tau_{wait} = 10T = 1ms \sim 1/\Delta f_{Lock\text{-}in}$.

B. Analysis of OI-RD Signals With FFT

It is known that magnitudes of various harmonics in (1) can be determined with a digital Fourier analysis in which the waveform is first digitized and then the harmonic magnitudes are obtained with a Fourier analysis of the digitized data [12]–[14]. In our present work, we digitize the light beam intensity at the photo-receiver with a data acquisition board (PCI-6281) from National Instrument. The maximum sampling frequency for PCI 6281 is $f_s = 625kHz$ ($T_s = 1/f_s$ is the sampling period). At this frequency, we take N data points from the wave form in (1). The N discrete data points are [15]

$$\begin{aligned} x_m(n) &= x_m(t)|_{t=nT_s} \\ &= I_m \cos(2\pi m f_{PEM} n T_s + \varphi_m)\ n = 0, \cdots, N-1 \end{aligned} \quad (5)$$

The standard discrete Fourier transformation of (5) yields a set of complex Fourier coefficients,

$$X_m(k) = \sum_{n=0}^{N-1} x_m(n)\, e^{-j\frac{2\pi}{N}kn} \quad (6)$$

$X_m(k)$ is the frequency domain signal at k of m^{th} harmonic. With Euler's formula, (6) can be expanded as

$$\begin{aligned} X_m(k) &= \sum_{n=0}^{N-1} I_m \cos\left(\frac{2\pi m f_{PEM}}{f_s} n + \varphi_m\right) \\ &\quad \times \left[\cos\left(\frac{2\pi}{N} kn\right) - j\sin\left(\frac{2\pi}{N} kn\right)\right] \\ &= \sum_{n=0}^{N-1} \frac{I_m}{2} \cos\left[2\pi\left(\frac{m f_{PEM}}{f_s} + \frac{k}{N}\right) n + \varphi_m\right] \\ &\quad + \sum_{n=0}^{N-1} \frac{I_m}{2} \cos\left[2\pi\left(\frac{m f_{PEM}}{f_s} - \frac{k}{N}\right) n + \varphi_m\right] \\ &\quad - j\sum_{n=0}^{N-1} \frac{I_m}{2} \sin\left[2\pi\left(\frac{m f_{PEM}}{f_s} + \frac{k}{N}\right) n + \varphi_m\right] \\ &\quad + j\sum_{n=0}^{N-1} \frac{I_m}{2} \sin\left[2\pi\left(\frac{m f_{PEM}}{f_s} - \frac{k}{N}\right) n + \varphi_m\right] \end{aligned} \quad (7)$$

When N is large, (7) is significantly non-zero when k equals a multiple of $N \times (f_{PEM}/f_s)$, namely, $k = m \times N \times (f_{PEM}/f_s)$. If N is such that $N \times (f_{PEM}/f_s)$ is an integer, we have for $m = 1$

$$X(k = N \times (f_{PEM}/f_s)) = \frac{N I_1}{2} e^{i\varphi_1} \quad (8)$$

For $m = 2$, we have

$$X(k = 2N \times (f_{PEM}/f_s)) = \frac{N I_2}{2} e^{i\varphi_2} \quad (9)$$

Thus I_1 and I_2 are determined as follows

$$I_1 = \frac{|X(N \times (f_{PEM}/f_s))|}{(N/2)} \quad (10a)$$

$$I_2 = \frac{|X(2N \times (f_{PEM}/f_s))|}{(N/2)} \quad (10b)$$

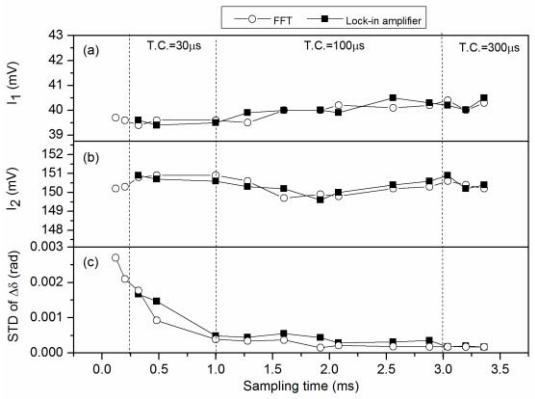

Fig. 2. (a) First harmonic amplitude I_1, (b) second harmonic amplitude I_2, and (c) standard deviation (STD) of $\Delta\delta$ analyzed simultaneously by an FFT analysis and a Lock-in amplifier vs. the sampling time. The sampling time is at least 10 times of the time constant (T.C.) used by the Lock-in amplifier.

In our present case, fs = 625 kHz and f_{PEM} = 50 kHz. To make $N \times (f_{PEM}/f_s) = M$ with M being an integer, we choose

$$N = 25 \times M \tag{11}$$

By sampling a wave-form I(t) N times at a frequency f_s, the sampling time is $\tau_{sampling} = NT_s = N/f_s$. To reduce the contribution of spectral leakage from frequency regions away from the vicinity of harmonics of interest, we use a Hanning window that provides an equivalent noise bandwidth (ENBW) of $\Delta f_{FFT} = 1.5/\left(\tau_{sampling}\right) = 1.5f_s/N$.

III. Results and Analysis

A. Comparisons of a Direct FFT Analysis With Lock-in Amplifier Analysis of OI-RD Signals

We compared the performances of the FFT analysis and the Lock-in amplifier measurement on the waveform of an OI-RD signal. The OI-RD signal is generated as follows. In Fig. 1, the light beam at 633 nm is polarization modulated and then reflected from the interface between the back surface of a glass slide and an aqueous solution. After an analyzer, the reflected light with an average power of 5 μW is detected with a photodiode and the photocurrent is converted to a voltage signal with a gain of 5×10^4 V/A. With the PEM modulation amplitude $\varphi_A = 1.63$ radians, amplitudes of the first and second harmonic components of the resultant voltage signal are 40 mV and 150 mV, respectively. For the FFT analysis, we use the maximum sampling frequency of 625 kHz for NI PCI 6281 board with an 18-bit A/D converter and a gain of 50 for the smallest sampling range of $\pm$ 0.1 V, and 14 different sampling number N (from 75 to 2100) for sets of digitized data. For the simultaneous Lock-in measurement, we use SR830 Digital Lock-in amplifier with the low pass filter set to a slope of 24 dB/oct . We choose the time constant T so that the wait time $\tau_{wait} \geq 10T$ is made equal to the sampling time $\tau_{sampling} = NT_s = N/f_s$ in the FFT analysis. As a result, the data acquisition times in both cases are kept the same. Fig. 2(a) and Fig. 2(b) shows that the amplitudes of harmonics measured in both analyses are essentially the same, thus the relevant parameter for comparison is the standard deviation of a harmonic.

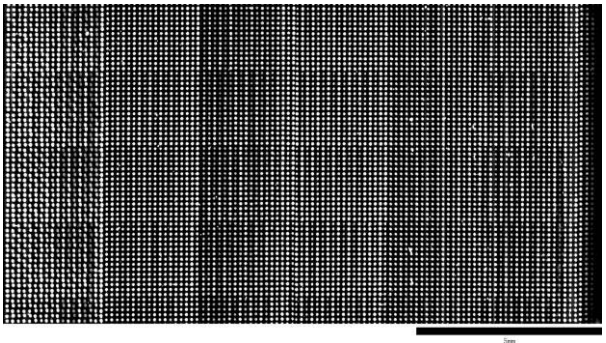

Fig. 3. A scanning OI-RD image of a BBSA microarray with 6,993 printed spots over an area of 28 mm $\times$ 16 mm obtained by the direct FFT analysis.

Fig. 2(c) shows the standard deviation (STD) of the OI-RD signal $\Delta\delta$ measured simultaneously with the FFT method and the Lock-in amplifiers for different sampling times $\tau_{sampling} = N/f_s$. In general, the STD of the first harmonic extracted from the FFT analysis are comparable to those measured with lock-in amplifiers for same sampling (wait) times. This shows that a modestly small OI-RD signal can be measured by using a direct FFT analysis instead of Lock-in amplifiers without sacrificing the signal-to-noise ratio (SNR).

B. Simultaneous Detection of Thousands of Biochemical Reactions on a Solid Support Analyzed With the Direct FFT Method

As a label-free biosensor, the OI-RD technique is now developed into a high-throughput platform for simultaneous detection of as many as tens of thousands biochemical reactions on a solid support [7], [16]–[18]. A scanning OI-RD microscope is used to acquire images of over 10,000 immobilized targets on the solid surface and to acquire as many binding curves of a solution-phase probe with these targets [19]. To illustrate the effectiveness of a direct FFT analysis of OI-RD data, we fabricated an array of 6,993 biotin-conjugated bovine serum albumin (BBSA) on an epoxy-functionalized glass surface. The array covers an area of 28 mm $\times$ 16 mm. Each fabricated spot is 150 μm in diameter and separated from its four neighboring spots by a center-to-center distance of 250 μm. With a scan step size of 20 μm in two orthogonal directions, we have $1500 \times 800 = 1.2 \times 10^6$ pixels in an image to scan, and $\sim 1.4 \times 10^4$ pixels (2×6993) for one time point of 6,993 simultaneously acquired binding curves. The factor of 2 comes from the need to acquire a reading midway between centers of two neighboring targets as the reference. An OI-RD image of the BBSA microarray in an aqueous buffer solution is shown in Fig. 3. The sampling time at each pixel is $\tau_{sampling} = N/f_s = 1$ms (fs = 625 kHz and N = 625). The total image acquisition time is 24 min, out of which 20 min is used for time spent on sampling 1.2×10^6 pixels.

We subsequently incubated the microarray in a solution of anti-biotin antibody at a concentration of 62.5 nM and measured the association-dissociation curves on all 6,993 immobilized BBSA targets. Fig. 4 shows a portion of 6,993 simultaneously acquired binding curves and the variation in the maximal value of kinetic curves is due to the variation in the surface density of the printed target [19].

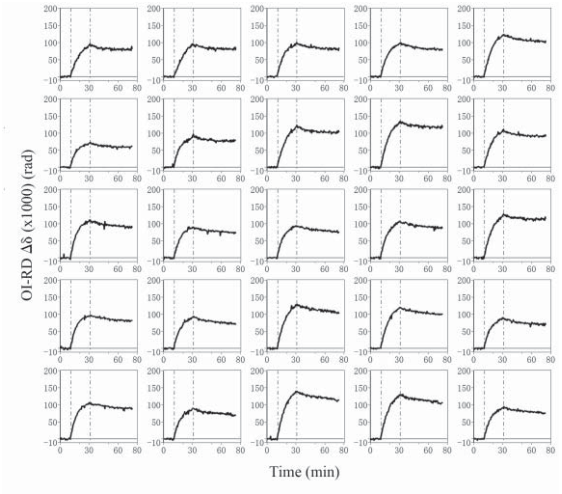

Fig. 4. A small portion of 6,993 simultaneously acquired association-dissociation curves acquired during incubation of the BBSA microarray and a solution of anti-biotin antibody. Vertical lines mark the starts of association and dissociation phases of the binding event, respectively.

Acquiring one time point for all 6,993 binding curves takes 24 s, out of which 14 s is spent on sampling $\sim 1.4 \times 10^4$ pixels and 10 s on moving stage and executing the software.

IV. Discussion and Conclusion

In present work we show that the method of direct FFT analysis can be used to replace bulky, costly Lock-in amplifiers for measuring harmonic components of waveforms with modest amplitudes (> micro volts). By using a data acquisition board (PCI-6281, National Instrument) with an 18-bit analog to digital converter (ADC), the detection sensitivity can be close to 0.8 μV according to specification of PCI-6281. On the noise introduced by the data acquisition board, there are three sources that contribute to the accuracy of the voltage detection: 1) Gain Error; 2) Offset Error; 3) random noise. By detecting harmonics in a periodic voltage signal away from the zero frequency, the effect of Offset Error is eliminated. By using the ratio of two harmonics as the final signal according to (4), the Gain Error is eliminated. We are left with only the random noise which is $V_n = 1 \times 10^{-5}/\sqrt{Hz}$ of the full scale. If we choose the scale on the board to maximize the second harmonic I_2 while choosing the modulation amplitude to make $J_1(\varphi_A) = 0.44$ and $J_2(\varphi_A) = 0.11$, we can achieve the minimum detectable OI-RD signal to $\Delta\delta = (V_n/I_2 \text{ (full scale)})\,(J_2(\varphi_A)/J_1(\varphi_A)) = 2.5 \times 10^{-6}\text{rad}/\sqrt{Hz}$. With an ENBW = 1000 Hz, the minimum detectable OI-RD signal is 7.9×10^{-5} rad.

By using the FFT analysis, it is also possible to reduce the data acquisition time in OI-RD at the expense of the signal-to-noise ratio. Fig. 2 shows that the minimal sampling time achievable with the FFT analysis is $\tau_{sampling} = N/f_s = 0.12$ ms ($f_s = 625$ kHz and $N = 75$) while the minimal time constant for measuring harmonics of the modulation frequency at 50 kHz is limited to $T = 0.03$ ms. As a result the minimal wait time is $\tau_{wait} = 10T = 0.3$ ms with a 24 dB/oct low pass filter. The minimal acquisition time for image and binding curves measurement with the FFT analysis is a factor of 2.5 less than the minimal time required with the Lock-in measurement. By optimizing the software architecture to reduce the time spent on software execution, it is possible to minimize the image acquisition time of large microarray to under 10 min, the time resolution for 10,000 binding curves measurement to 10 s.

In conclusion, direct FFT analysis provides comparable performance as Lock-in measurement for signals larger than micro-volts with advantages of simplicity, low cost, compact design, and flexibility which make it possible to develop the OI-RD platform for highly parallel ultrathin film detection into a viable instrumentation.

References

[1] A. Fried, M. Fejer, and A. Kapitulnik, "A scanning, all-fiber Sagnac interferometer for high resolution magneto-optic measurements at 820 nm," *Rev. Sci. Instrum.*, vol. 85, p. 103707, Oct. 2014.

[2] C. Zhu *et al.*, "Calibration of oblique-incidence reflectivity difference for label-free detection of a molecular layer," *Appl. Opt.*, vol. 55, pp. 9459–9466, Nov. 2016.

[3] X. D. Zhu, S. Wicklein, F. Gunkel, R. Xiao, and R. Dittmann, "*In situ* optical characterization of $LaAlO_3$ epitaxy on $SrTiO_3(001)$," *Europhys. Lett.*, vol. 109, no. 3, p. 37006, 2015.

[4] W. Schwarzacher, J. Gray, and X. D. Zhu, "Oblique incidence reflectivity difference as an *in situ* probe of Co electrodeposition on polycrystalline Au," *Electrochem. Solid State Lett.*, vol. 6, no. 5, pp. C73–C76, 2003.

[5] G. Y. Wu *et al.*, "Pb electrodeposition on polycrystalline Cu in the presence and absence of Cl^-: A combined oblique incidence reflectivity difference and *in situ* AFM study," *Surf. Sci.*, vol. 601, no. 8, pp. 1886–1891, 2007.

[6] Y. Fei *et al.*, "Characterization of receptor binding profiles of influenza a viruses using an ellipsometry-based label-free glycan microarray assay platform," *Biomolecules*, vol. 5, no. 3, pp. 1480–1498, 2015.

[7] J. P. Landry, Y. Fei, X. Zhu, Y. Ke, G. Yu, and P. Lee, "Discovering small molecule ligands of vascular endothelial growth factor that block VEGF–KDR binding using label-free microarray-based assays," *Assay Drug Develop. Technol.*, vol. 11, no. 5, pp. 326–332, Jun. 2013.

[8] X. Guo *et al.*, "Characterization of protein expression levels with label-free detected reverse phase protein arrays," *Anal. Biochem.*, vol. 509, pp. 67–72, Sep. 2016.

[9] C.-Y. Han and Y.-F. Chao, "Photoelastic modulated imaging ellipsometry by stroboscopic illumination technique," *Rev. Sci. Instrum.*, vol. 77, p. 023107, Feb. 2006.

[10] O. Acher, E. Bigan, and B. Drévillon, "Improvements of phase-modulated ellipsometry," *Rev. Sci. Instrum.*, vol. 60, pp. 65–77, Jan. 1989.

[11] S. Vallon, E. Compain, and B. Drévillon, "Improvements of Fourier transform phase-modulated ellipsometry," *Rev. Sci. Instrum.*, vol. 66, pp. 3269–3272, May 1995.

[12] M. V. Khazimullin and Y. A. Lebedev, "Fourier transform approach in modulation technique of experimental measurements," *Rev. Sci. Instrum.*, vol. 81, p. 043110, Apr. 2010.

[13] R. Petkovšek, J. Petelin, J. Možina, and F. Bammer, "Fast ellipsometric measurements based on a single crystal photo-elastic modulator," *Opt. Exp.*, vol. 18, pp. 21410–21418, Sep. 2010.

[14] B. Drevillon, J. Perrin, R. Marbot, A. Violet, and J. L. Dalby, "Fast polarization modulated ellipsometer using a microprocessor system for digital Fourier analysis," *Rev. Sci. Instrum.*, vol. 53, no. 7, pp. 969–977, 1982.

[15] J. Kauppinen and J. Partanen, "Discrete Fourier transform," in *Fourier Transforms in Spectroscopy*. Hoboken, NJ, USA: Wiley, 2002, pp. 35–48.

[16] J. P. Landry, Y. Ke, G.-L. Yu, and X. D. Zhu, "Measuring affinity constants of 1450 monoclonal antibodies to peptide targets with a microarray-based label-free assay platform," *J. Immunol. Methods*, vol. 417, pp. 86–96, Feb. 2015.

[17] J. Wang *et al.*, "Epigallocatechin-3-gallate enhances ER stress-induced cancer cell apoptosis by directly targeting PARP16 activity," *Cell Death Discovery*, vol. 3, Jul. 2017, Art. no. 17034.

[18] C. Zhu *et al.*, "Developing an efficient and general strategy for immobilization of small molecules onto microarrays using isocyanate chemistry," *Sensors*, vol. 16, no. 3, p. 378, Mar. 2016.

[19] J. P. Landry, Y. Fei, and X. Zhu, "Simultaneous measurement of 10,000 protein-ligand affinity constants using microarray-based kinetic constant assays," *Assay Drug Develop. Technol.*, vol. 10, pp. 250–259, Jun. 2012.